CrystEngComm

PAPER

View Article Online
View Journal | View Issue

Cite this: *CrystEngComm*, 2018, **20**, 6995

Insights into inorganic buffer layer-assisted *in situ* fabrication of MOF films with controlled microstructures†

Yi Liu, [a] Ryotaro Matsuda, *[bc] Shinpei Kusaka, [d] Akihiro Hori, [b] Yunsheng Ma [b] and Susumu Kitagawa*[d]

Received 2nd October 2018,
Accepted 10th October 2018

DOI: 10.1039/c8ce01681j

rsc.li/crystengcomm

In this study, it was demonstrated that the introduction of Co–Al/Mg–Al hydrotalcite-like compound buffer layers on porous α-Al_2O_3 substrates enabled effective manipulation of the microstructure of ZIF-7 films so that metal ions located in the inorganic buffer layers were not necessarily identical with those residing in the MOF crystals. Moreover, zinc sources were found to exert a significant influence on the final microstructure of the prepared ZIF-7 films. In addition to ZIF-7, well-intergrown ZIF-8 and HKUST-1 films could also be *in situ* grown on diverse HTlc buffer layer-modified α-Al_2O_3 substrates, which convincingly demonstrated the generality of this strategy for the facile preparation of qualified MOF films/membranes.

Introduction

Metal–organic frameworks (MOFs) in the form of thin films have shown unprecedented opportunities and promise in the fields of luminescence,[1–3] QCM-based VOC vapor sensing,[4–6] optoelectronics,[7] gas separation[8–11] and catalysis[12,13] due to their unique structural flexibility, tailor-made functionalities, large surface areas and adjustable pore apertures.[14] Nevertheless, one of the challenging tasks facing MOF film fabrication remains the low-affinity interactions between the chemically inert substrate surface and the MOF crystals, which inevitably gives rise to a low heterogeneous nucleation density.[15,16] Therefore, incorporation of additional functional groups into the substrate surface has become indispensable to improve their binding affinity. A variety of organic compounds, including imidazole derivatives,[17] PMMA,[18] APTES,[19] IPTES,[20] and PDA,[21] have proven effective for substrate activation. In contrast, relatively less attention has been paid to pure inorganic modifiers which, in effect, may show superior performance in terms of robustness,[22] substrate compatibility, thermal stability and environmental friendliness. For instance, well-intergrown ZIF-8,[23] ZIF-71 (ref. 24) and ZIF-78 (ref. 25) membranes could be synthesized on porous ZnO or ZnO-modified α-Al_2O_3 substrates; very recently it was demonstrated that ZIF-67 ($[Co(MeIm)_2]_n$) films could be *in situ* grown on Co–Al LDH-modified Ni substrates and serve as the precursor for supercapacitor electrodes;[26] while H_2-selective $[Cu_3(BTC)_2]$ membranes could be fabricated on CuO/Cu nets[27] or Cu/Ni_3S_2/Ni foams[28] by *in situ* solvothermal reactions. It should be noted, however, that in almost all cases metal ions present in inorganic modifiers are identical with those in MOF frameworks. Although some authors tried elucidating this issue in a recent study, the use of conducting substrates and the requirement for electrodeposition of inorganic buffer layers have restricted the potential widespread application.[29] Thus, it becomes essential for us to elucidate the principle of inorganic functionalization to bypass such restrictions.

Besides, there is also an increasing demand for facile methods allowing more precise control over the microstructure (like grain size and shape, film thickness and preferred orientation) of MOF films which, however, are mainly based on trial and error and have turned out to be very sophisticated. Taking ZIF-7, a representative of MOF materials, as an example, at present ZIF-7 films with diverse microstructures have to be fabricated by *in situ* growth, polyethylenimine (PEI)-assisted seeding,[16] microwave-assisted secondary growth,[16] benzimidazole covalent functionalization, electrospray deposition[30] or the use of sodium formate as a deprotonation agent.[17] Comparatively speaking, *in situ* growth is more preferable for industrial mass production due to its simplicity.[31] Therefore, it became highly desirable to enable effective manipulation of microstructures of MOF films *via* a facile *in situ* growth method.

[a] *State Key Laboratory of Fine Chemicals, School of Chemical Engineering, Dalian University of Technology, 116024, Dalian, China*
[b] *Department of Chemistry and Biotechnology, School of Engineering, Nagoya University, Furo-cho, Chikusa-ku, 464-8603, Nagoya, Japan.*
E-mail: ryotaro.matsuda@chembio.nagoya-u.ac.jp
[c] *PRESTO, Japan Science and Technology Agency (JST), 4-1-8 Honcho, 332-0012, Kawaguchi, Japan*
[d] *Institute for Integrated Cell-Material Sciences (WPI-iCeMS), Kyoto University, Katsura, Nishikyo-ku, 615-8510, Kyoto, Japan.*
E-mail: kitagawa@icems.kyoto-u.ac.jp

† Electronic supplementary information (ESI) available. See DOI: 10.1039/c8ce01681j

Hydrotalcite-like compounds (HTlcs) are a typical representative of anionic clays consisting of positively charged brucite-like layers and charge-compensating anions located in interlayer galleries. Compositional flexibility in both positively charged layers and charge-balancing anions gives rise to a functional diversity.[32] In view of our previous demonstration of high-affinity interactions between HTlc buffer layers and MOF films,[33–35] herein we further showed that microstructures of ZIF-7 films could be precisely controlled by proper manipulation of structure-related parameters of HTlc buffer layers (schematically shown in Fig. 1). Of particular note is that metal ions present in buffer layers and MOF films are different, which demonstrates convincingly that a much wider range of inorganic compounds are appropriate for a significant enhancement of nucleation and growth of MOF films.

Experimental

Growth of ZIF-7 films on bare α-Al_2O_3 substrates

0.57 g $Zn(NO_3)_2{\cdot}6H_2O$ (99.9 wt%, Wako) and 0.31 g benzimidazole (98.0 wt%, TCI) were dissolved in 30 ml DMF (99.5 wt%, nacalai tesque). After vigorous stirring at room temperature for 10 min, a bare α-Al_2O_3 substrate (Fraunhofer Institut, Germany) was placed into a 50 ml Teflon-lined stainless steel vessel, and 35 ml of the precursor solution was poured into the vessel. The vessel was sealed and put into a convection oven with the temperature preheated to 100 °C. After 20 h, the vessel was taken out and cooled to room temperature. Finally the film was taken out, washed with DMF and dried in air.

Growth of Co–Al–CO_3 HTlc buffer layers on α-Al_2O_3 substrates

The precursor solution was prepared by mixing 0.54 g of $Co(NO_3)_2{\cdot}6H_2O$ (98 wt%, Aldrich), 0.35 g $Al(NO_3)_3{\cdot}9H_2O$ (98.0 wt%, nacalai tesque) and 1.6 g urea (99.0 wt%, Wako) with 100 ml DDI water. Then a porous α-Al_2O_3 substrate was vertically placed into a 50 ml Teflon-lined stainless steel vessel and 35 ml of the precursor solution was poured into the vessel. The vessel was sealed and put into a convection oven with the temperature preheated to 120 °C. After 20 h, the vessel was taken out and cooled to room temperature. Finally, the substrate was taken out and washed with DDI water.

Growth of ZIF-7 films on Co–Al–CO_3 HTlc buffer layer-modified α-Al_2O_3 substrates

This procedure is similar to the synthesis of ZIF-7 films on bare α-Al_2O_3 substrates except that Co–Al–CO_3 HTlc buffer layer-modified α-Al_2O_3 substrates were used.

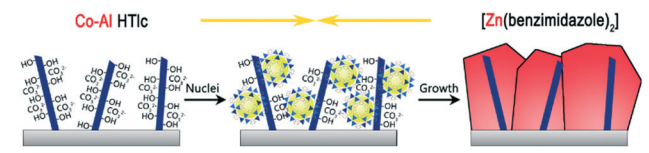

Fig. 1 Schematic illustration of *in situ* solvothermal synthesis of qualified ZIF-7 films on Co–Al HTlc buffer layer-modified α-Al_2O_3 substrates.

Growth of Mg–Al–CO_3 HTlc buffer layers on α-Al_2O_3 substrates

The precursor solution was prepared by mixing 0.48 g of $Mg(NO_3)_2{\cdot}6H_2O$ (98 wt%, Aldrich), 0.35 g $Al(NO_3)_3{\cdot}9H_2O$ and 1.6 g urea with 100 ml DDI water. Then, a porous α-Al_2O_3 substrate was placed into a 50 ml Teflon-lined stainless steel vessel, and 35 ml of the precursor solution was poured into the vessel. The vessel was sealed and put into a convection oven with the temperature preheated to 120 °C. After 20 h, the vessel was taken out and cooled to room temperature. Finally, the substrate was taken out and washed with water.

Growth of Mg–Al–CO_3 HTlc buffer layers on γ-Al_2O_3 substrates

This procedure is similar to the synthesis of Mg–Al–CO_3 HTlc on α-Al_2O_3 substrates except that γ-Al_2O_3 substrates are used instead.

Growth of ZIF-7 films on Mg–Al–CO_3 HTlc buffer layer-modified α-Al_2O_3 substrates

This procedure is similar to the synthesis of ZIF-7 films on bare α-Al_2O_3 substrates except that Mg–Al–CO_3 HTlc buffer layer-modified α-Al_2O_3 substrates were used instead.

Growth of ZIF-7 films on Mg–Al–CO_3 HTlc buffer layer-modified γ-Al_2O_3 substrates

This procedure is similar to the synthesis of ZIF-7 films on bare α-Al_2O_3 substrates except that Mg–Al–CO_3 HTlc buffer layer-modified γ-Al_2O_3 substrates were used instead.

Growth of ZIF-7 films on Co–Al–CO_3 HTlc buffer layer-modified α-Al_2O_3 substrates with $ZnCl_2$ as the zinc source

0.41 g $ZnCl_2$ (98.0 wt%, Wako), 0.38 g benzimidazole and 1.02 g diethylamine (99.0 wt%, TCI) were dissolved in 30 ml DMF. After vigorous stirring at room temperature for 10 min, a Co–Al–CO_3 HTlc buffer layer-modified α-Al_2O_3 substrate was vertically placed into a 50 ml Teflon-lined stainless steel vessel, and 30 ml of the precursor solution was poured into the vessel. The vessel was sealed and put into a convection oven with the temperature preheated to 100 °C. After an elapsed time of 20 h, the vessel was taken out and naturally cooled to room temperature in air. Finally, the film was taken out, washed with DMF water and dried in air.

Growth of ZIF-7 films on Co–Al–CO_3 HTlc buffer layer-modified α-Al_2O_3 substrates with $ZnBr_2$ as the zinc source

0.68 g $ZnBr_2$ (99.9 wt%, Wako), 0.38 g benzimidazole and 1.02 g diethylamine were dissolved in 30 ml DMF. After vigorous stirring at room temperature, a Co–Al–CO_3 HTlc buffer layer-modified α-Al_2O_3 substrate was placed into a 50 ml Teflon-lined stainless steel vessel, and 30 ml of the precursor solution was poured into the vessel. The vessel was sealed and then put into a convection oven with the temperature preheated to 100 °C. After 20 h, the vessel was taken out and cooled to room temperature in air. Finally, the film was taken out, washed with DMF water and dried in air.

Growth of ZIF-7 films on Co–Al–CO_3 HTlc buffer layer-modified α-Al_2O_3 substrates with ZnI_2 as the zinc source

0.96 g ZnI_2 (99.0 wt%, nacalai tesque), 0.38 g benzimidazole and 1.02 g diethylamine were dissolved in 30 ml DMF. After vigorous stirring at room temperature, a Co–Al–CO_3 HTlc buffer layer-modified α-Al_2O_3 substrate was placed into a 50 ml Teflon-lined stainless steel vessel, and 30 ml of the precursor solution was poured into the vessel. The vessel was sealed and put into a convection oven with the temperature preheated to 100 °C. After 20 h, the vessel was taken out and cooled to room temperature. Finally, the film was taken out, washed with DMF water and dried in air.

Results and discussion

Effects of Co–Al HTlc buffer layer modification on the microstructure of ZIF-7 films

Initially we tried to prepare ZIF-7 films on bare α-Al_2O_3 substrates by *in situ* solvothermal growth with $Zn(NO_3)_2{\cdot}6H_2O$ as the metal ion source. After the synthesis, large ZIF-7 crystals (grain size ~10 μm) were readily attached to the substrate (Fig. 2a and b and 3a). Nevertheless, substantial intercrystalline defects remained in the film due to a relatively low nucleation density. To enhance the chemical affinity between the substrates and the ZIF-7 crystals, before solvothermal growth, a Co–Al HTlc buffer layer was introduced to the substrate by *in situ* hydrothermal growth. As shown in Fig. 2c, the prepared HTlc buffer layer showed a typical plate-like morphology with an average grain size of 4 μm. The mutual distances between adjacent HTlc plates were ~2 μm (Fig. 2c and d). A high length-to-width ratio of Co–Al HTlc crystals was potentially desirable for substrate modification due to a maximized exposure of surface functional groups as well as minimized mass transfer barrier. The Co/Al ratio was estimated to be 1.28 based on energy-dispersive X-ray spectroscopy (EDXS) measurement (shown in Fig. S1 and S2†). The powder X-ray diffraction (PXRD) pattern further showed distinguishable diffraction peaks at 2θ values of 11.6° and 23.1°, which were coincident with the {003} and {006} crystal planes of the CO_3^{2-} intercalated Co–Al HTlc phase (Fig. 3b; the PXRD pattern is shown in Fig. S3†).[36,37]

In the next step, ZIF-7 films were *in situ* synthesized on Co–Al HTlc buffer layer-modified α-Al_2O_3 substrates. As shown in Fig. 2e, the prepared ZIF-7 film was well intergrown. Moreover, the grain size and film thickness had been significantly reduced to ~2 μm (Fig. 2e) and 5 μm (Fig. 2f). This can be attributed to the mutual electron donor (benzimidazole N atoms and interlayer OH^-/CO_3^{2-} anions)–acceptor (Co^{2+}, Al^{3+} and Zn^{2+} ions) interactions between the Co–Al HTlc and the ZIF-7 framework.[38,39] The existence of –OH/–CO_3^{2-} functional groups in the Co–Al HTlc buffer layer could be further confirmed by the FT-IR spectra (shown in Fig. S4†).[37]

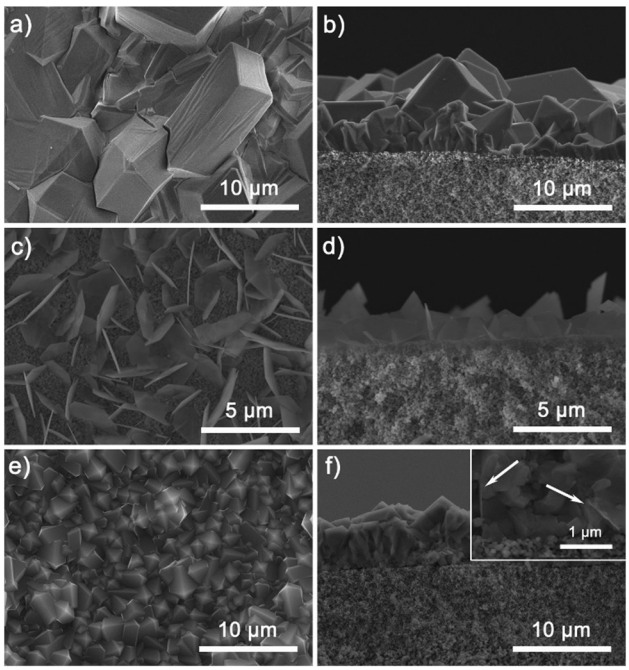

Fig. 2 SEM images of (a and b) ZIF-7 films prepared on bare α-Al_2O_3 substrates by *in situ* solvothermal growth; (c and d) Co–Al HTlc buffer layers *in situ* grown on α-Al_2O_3 substrates; and (e and f) ZIF-7 films prepared on Co–Al HTlc buffer layer-modified α-Al_2O_3 substrates by *in situ* solvothermal growth. Inset: Enlarged cross-sectional SEM image at the ZIF-7 film–substrate interface. White arrows: Co–Al HTlc crystals.

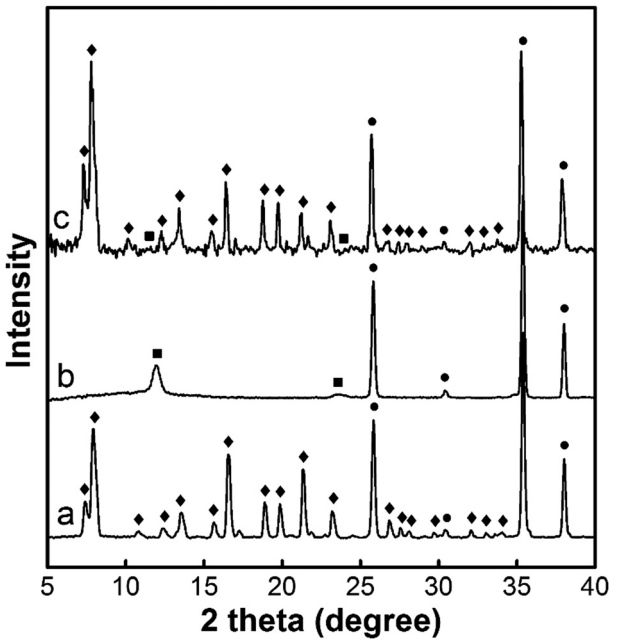

Fig. 3 XRD patterns of (a) ZIF-7 films prepared on bare α-Al_2O_3 substrates by *in situ* solvothermal growth; (b) Co–Al HTlc buffer layers *in situ* grown on α-Al_2O_3 substrates; and (c) ZIF-7 films prepared on Co–Al HTlc buffer layer-modified α-Al_2O_3 substrates by *in situ* solvothermal growth. Peaks marked with rhombuses, squares and dots represent diffraction peaks from the ZIF-7 film, Co–Al HTlc buffer layer and α-Al_2O_3 substrate, respectively.

Effects of zinc source on the microstructure of ZIF-7 films

Besides buffer layers, zinc sources were found to exert a significant influence on the final microstructure of ZIF-7 films. As shown in Fig. 4, rod-like ZIF-7 crystals were formed and spontaneously attached to Co–Al HTlc buffer layer-modified substrates in case $ZnCl_2$ (Fig. 4a and b)[40] or $ZnBr_2$ (Fig. 4c and d) were employed as the zinc source. Moreover, it was observed that not only the diameter of the ZIF-7 microrods synthesized from $ZnBr_2$ (Fig. 4c) was three times larger than those from $ZnCl_2$ (Fig. 4a), but also they were more closely packed with each other. Cross-sectional SEM images of both prepared ZIF-7 films (Fig. 4b and d) indicated that most ZIF-7 micro-/nano-rods should be vertically aligned on the substrate, which could be interpreted by the "evolution selection" growth mechanism developed by van der Drift in the interpretation of the preferred orientation of a vapor-deposited PbO layer.[41] Of particular note, the use of ZnI_2 as the zinc source unexpectedly resulted in the formation of 50-nm-sized ZIF-7 nanocrystals (shown in Fig. S5†) followed by their uniform *in situ* deposition on Co–Al HTlc buffer layer-modified substrates (Fig. 4e and f), which has never been reported in the literature. PXRD patterns further confirmed that all prepared films indeed belonged to the ZIF-7 phase (shown in Fig. S6†).

Morphological differences among ZIF-7 films could be partially interpreted by the hard–soft acid–base (HSAB) theory, in which $Cl^-/Br^-/I^-$ are classified as hard/intermediate/soft bases, respectively; while Zn^{2+} are defined as intermediate acids.[40] Since intermediate acids Zn^{2+} tend to form stronger bonds with intermediate bases (Br^-), as a result, heterogeneous nucleation of ZIF-7 on Co–Al HTlc-modified substrates is inhibited, which in turn provides enough space for morphology evolvement of ZIF-7 nuclei and ultimately leads to the formation of ZIF-7 films with large grain size and well-developed facets. In contrast, relatively weak interactions between Zn^{2+} (intermediate acids) and Cl^- (hard bases)/I^- (soft bases) give rise to enhanced heterogeneous nucleation and therefore relatively smaller grain size. Our deduction could be further confirmed by a recent study which employed $ZnCl_2$, $ZnBr_2$ and ZnI_2 as zinc sources for the preparation of ZIF-8 crystals.[42] The fact that the largest ZIF-8 nanocrystals were obtained with $ZnBr_2$ as the zinc source was also interpreted based on the HSAB theory.

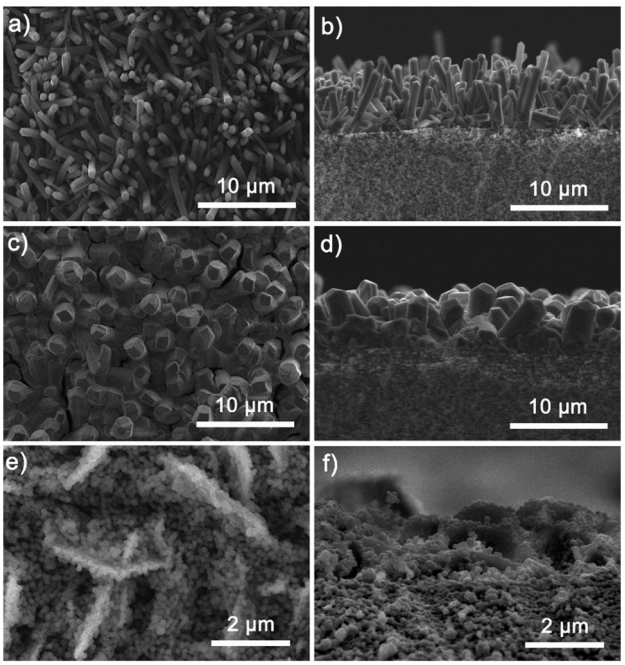

Fig. 4 SEM images of ZIF-7 films prepared on Co–Al HTlc buffer layer-modified α-Al_2O_3 substrates by *in situ* solvothermal growth with (a and b) $ZnCl_2$, (c and d) $ZnBr_2$ and (e and f) ZnI_2 as zinc sources.

Effects of HTlc buffer layer morphology on the microstructure of ZIF-7 films

Competent buffer layers are by no means confined to Co–Al HTlc buffer layers. In addition, we further prepared Mg–Al HTlc buffer layers composed of relatively sparsely distributed HTlc plates (Fig. 5a) on which ZIF-7 films with a grain size of 5–10 μm were *in situ* fabricated (Fig. 5b). Moreover, it was demonstrated that the morphology of the Mg–Al HTlc buffer layers exerted a significant influence on the final morphology of the prepared ZIF-7 films. For easy reference, Mg–Al HTlc buffer layers which consisted of more closely packed HTlc plates (Fig. 5c) were further *in situ* fabricated on porous γ-Al_2O_3 substrates. As indicated by the EDXS pattern, the Mg/Al ratio of Mg–Al HTlc buffer layers grown on α-Al_2O_3 substrates was estimated to be ~2.1 (shown in Fig. S7†). After *in situ* solvothermal synthesis, well-intergrown ZIF-7 films with a significantly reduced grain size were prepared (grain size ~1 μm, shown in Fig. 5d). This could be reasonably attributed to a remarkably increased number of active nucleation sites on Mg–Al HTlc buffer layer-modified substrates.

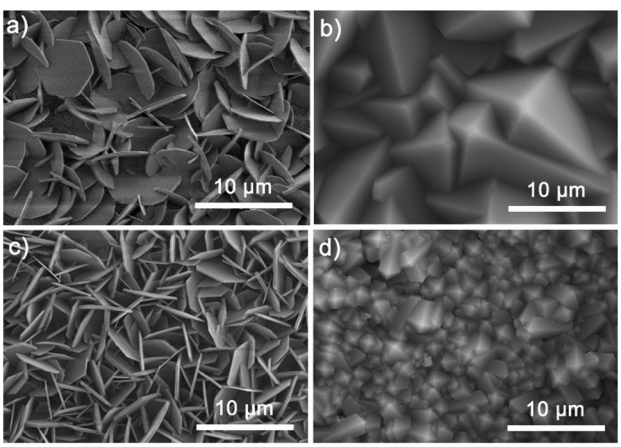

Fig. 5 SEM images of (a) Mg–Al HTlc buffer layers prepared on α-Al_2O_3 substrates, (b) ZIF-7 films prepared on Mg–Al HTlc buffer layer-modified α-Al_2O_3 substrates by *in situ* solvothermal growth, (c) Mg–Al HTlc buffer layers prepared on γ-Al_2O_3 substrates and (d) ZIF-7 films prepared on Mg–Al HTlc buffer layer-modified γ-Al_2O_3 substrates by *in situ* solvothermal growth.

All these results demonstrated that it was possible to adjust precisely microstructures of MOF films by judicious manipulation of the structure-related parameters of inorganic buffer layers aside from various solvothermal reaction parameters (like chemical composition of precursors, reaction time and temperature).

It should be emphasized that metal ions present in both HTlc buffer layers and the ZIF-7 framework are distinct, which unambiguously confirms that metal ions residing in inorganic modifiers are not necessarily identical with those in MOF frameworks, and there are no specific criteria for choosing inorganic buffer layers. This implies that in effect, a wide range of inorganic compounds are potentially competent buffer layers for promotion of nucleation and growth of MOF crystals.

Adhesion strength and reproducibility of ZIF-7 films

Strong adhesion of MOF crystals to the substrate surface is of vital importance for their practical applications. Herein, ultrasonic testing was carried out to evaluate the adhesion strength of ZIF-7 films. It was found that after 30 minutes of ultrasonic treatment, the prepared ZIF-7 film remained intact and firmly attached to the substrate (shown in Fig. 6). The reinforced mechanical stability of the ZIF-7 film can be attributed to the extra binding strength stemming from the intermediate HTlc network as suggested by previous studies.[22,43]

The prepared MOF films exhibited high reproducibility in case uniform and continuous HTlc buffer layers could be firmly attached to the substrates. To confirm this assumption, in parallel we prepared six ZIF-7 films on Co–Al HTlc buffer layer-modified α-Al_2O_3 substrates, and SEM results showed that all ZIF-7 films were well intergrown on a large scale.

Generality of the developed strategy

Our approach was confined not only to ZIF-7 film synthesis. With this method, well-intergrown ZIF-8 films could also be fabricated on both Co–Al and Mg–Al HTlc buffer layer-modified α-Al_2O_3 substrates (shown in Fig. 7). In contrast, ZIF-8 grains were only sparsely distributed on bare α-Al_2O_3 substrates in the case of direct crystallization as revealed in previous studies. In addition, we further confirmed that continuous HKUST-1 films could be *in situ* grown on Zn–Al LDH

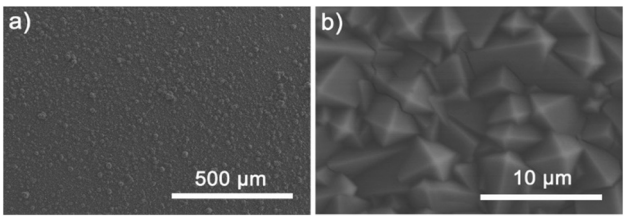

Fig. 6 (a and b) SEM images of the ZIF-7 film after ultrasonic treatment in methanol solvent for 30 min. Note: Cracks in (b) were spontaneously generated during the SEM observation.

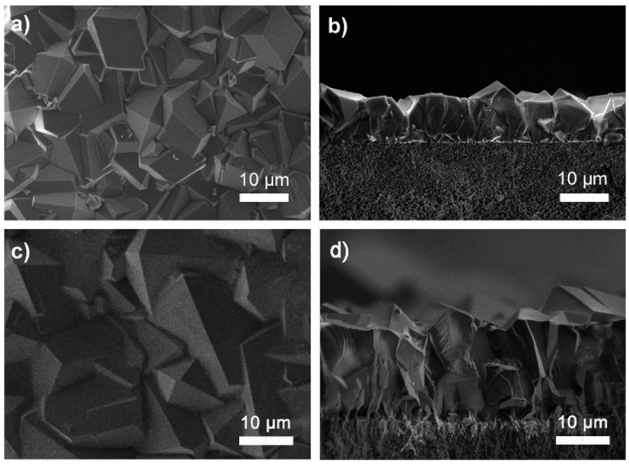

Fig. 7 SEM images of (a and b) ZIF-8 films prepared on Co–Al HTlc buffer layer-modified α-Al_2O_3 substrates by *in situ* solvothermal growth; (c and d) ZIF-8 films prepared on Mg–Al HTlc buffer layer-modified α-Al_2O_3 substrates by *in situ* solvothermal growth.

buffer layer-modified γ-Al_2O_3 substrates (shown in Fig. S8†), therefore demonstrating that this approach could be generalized to significantly promote nucleation and growth of diverse MOF films.

Conclusions

In this study we synthesized ZIF-7 films with diverse microstructures (including grain size, crystal morphology, film thickness and preferred orientation) on Co–Al/Mg–Al HTlc buffer layer-modified substrates by *in situ* solvothermal reaction. It is demonstrated that metal ions present in inorganic buffer layers and MOF films are not necessarily identical. Thus, the scope of inorganic compounds potentially appropriate for surface activation of substrates can be greatly expanded. Moreover, our concept is potentially preferable for mass production of MOF films since the microstructure of MOF films can be easily controlled simply *via* a facile *in situ* growth method. This can be realized simply by precisely tuning structure-related parameters of inorganic buffer layers. In addition, the influence of zinc sources on the final microstructures of ZIF-7 films was systematically investigated. We firmly believe that the concept developed here could be potentially beneficial for efficient fabrication of diverse advanced MOF-based hybrid materials.

Conflicts of interest

There are no conflicts to declare.

Acknowledgements

This work is supported by the PRESTO (Grant No. JPMJPR141C), CREST (Grant No. JPMJCR17I3) and ACCEL (Grant No. JPMJAC1302) of the Japan Science and Technology Agency (JST), and a JSPS KAKENHI Grant-in-Aid for Young Scientists (A) (Grant No. 16H06032). The authors are grateful to

Thousand Youth Talents Program and the National Natural Science Foundation of China (21176231) for the financial support. Y. M. acknowledges the financial support by the NSF of Jiangsu Provence (No. 14KJA150001) China and The Six Talent Peaks Project in Jiangsu Province (2013XCL-023).

References

1 H. P. Liu, H. M. Wang, T. S. Chu, M. H. Yu and Y. Y. Yang, *J. Mater. Chem. C*, 2014, **2**, 8683.
2 Z. S. Dou, J. C. Yu, Y. J. Cui, Y. Yang, Z. Y. Wang, D. R. Yang and G. D. Qian, *J. Am. Chem. Soc.*, 2014, **136**, 5527.
3 X. Shen and B. Yan, *Dalton Trans.*, 2015, **44**, 1875.
4 M. Tu, S. Wannapaiboon, K. Khaletskaya and R. A. Fischer, *Adv. Funct. Mater.*, 2015, **25**, 4470.
5 S. Wannapaiboon, M. Tu, K. Sumida, K. Khaletskaya, S. Furukawa, S. Kitagawa and R. A. Fischer, *J. Mater. Chem. A*, 2015, **3**, 2338.
6 K. Khaletskaya, S. Turner, M. Tu, S. Wannapaiboon, A. Schneemann, R. Meyer, A. Ludwig, G. Van Tendeloo and R. A. Fischer, *Adv. Funct. Mater.*, 2014, **24**, 4804.
7 Y. N. Wu, F. T. Li, Y. X. Xu, W. Zhu, C. A. Tao, J. C. Cui and G. T. Li, *Chem. Commun.*, 2011, **47**, 10094.
8 Y. Peng, Y. S. Li, Y. J. Ban, H. Jin, W. M. Jiao, X. L. Liu and W. S. Yang, *Science*, 2014, **346**, 1356.
9 S. L. Qiu, M. Xue and G. S. Zhu, *Chem. Soc. Rev.*, 2014, **43**, 6116.
10 H. Bux, F. Y. Liang, Y. S. Li, J. Cravillon, M. Wiebcke and J. Caro, *J. Am. Chem. Soc.*, 2009, **131**, 16000.
11 A. J. Brown, N. A. Brunelli, K. Eum, F. Rashidi, J. R. Johnson, W. J. Koros, C. W. Jones and S. Nair, *Science*, 2014, **345**, 72.
12 I. Hod, M. D. Sampson, P. Deria, C. P. Kubiak, O. K. Farha and J. T. Hupp, *ACS Catal.*, 2015, **5**, 6302.
13 C. W. Kung, J. E. Mondloch, T. C. Wang, W. Bury, W. Hoffeditz, B. M. Klahr, R. C. Klet, M. J. Pellin, O. K. Farha and J. T. Hupp, *ACS Appl. Mater. Interfaces*, 2015, **7**, 28223.
14 S. Kitagawa, R. Kitaura and S. Noro, *Angew. Chem., Int. Ed.*, 2004, **43**, 2334.
15 M. Shah, M. C. McCarthy, S. Sachdeva, A. K. Lee and H. K. Jeong, *Ind. Eng. Chem. Res.*, 2012, **51**, 2179.
16 Y. S. Li, F. Y. Liang, H. Bux, A. Feldhoff, W. S. Yang and J. Caro, *Angew. Chem., Int. Ed.*, 2010, **49**, 548.
17 M. C. McCarthy, V. Varela-Guerrero, G. V. Barnett and H. K. Jeong, *Langmuir*, 2010, **26**, 14636.
18 T. Ben, C. J. Lu, C. Y. Pei, S. X. Xu and S. L. Qiu, *Chem. – Eur. J.*, 2012, **18**, 10250.
19 A. S. Huang, W. Dou and J. Caro, *J. Am. Chem. Soc.*, 2010, **132**, 15562.
20 S. Tanaka, T. Shimada, K. Fujita, Y. Miyake, K. Kida, K. Yogo, J. F. M. Denayer, M. Sugita and T. Takewaki, *J. Membr. Sci.*, 2014, **472**, 29.
21 Q. Liu, N. Y. Wang, J. Caro and A. S. Huang, *J. Am. Chem. Soc.*, 2013, **135**, 17679.
22 X. F. Zhang, Y. G. Liu, S. H. Li, L. Y. Kong, H. O. Liu, Y. S. Li, W. Han, K. L. Yeung, W. D. Zhu, W. S. Yang and J. S. Qiu, *Chem. Mater.*, 2014, **26**, 1975.
23 X. F. Zhang, Y. Q. Liu, L. Y. Kong, H. O. Liu, J. S. Qiu, W. Han, L. T. Weng, K. L. Yeung and W. D. Zhu, *J. Mater. Chem. A*, 2013, **1**, 10635.
24 X. L. Dong and Y. S. Lin, *Chem. Commun.*, 2013, **49**, 1196.
25 X. L. Dong, K. Huang, S. N. Liu, R. F. Ren, W. Q. Jin and Y. S. Lin, *J. Mater. Chem.*, 2012, **22**, 19222.
26 Y. B. Dou, J. Zhou, F. Yang, M. J. Zhao, Z. R. Nie and J. R. Li, *J. Mater. Chem. A*, 2016, **4**, 12526.
27 H. L. Guo, G. S. Zhu, I. J. Hewitt and S. L. Qiu, *J. Am. Chem. Soc.*, 2009, **131**, 1646.
28 Y. X. Sun, F. Yang, Q. Wei, N. X. Wang, X. Qin, S. K. Zhang, B. Wang, Z. R. Nie, S. L. Ji, H. Yan and J. R. Li, *Adv. Mater.*, 2016, **28**, 2374.
29 S. Zhou, Y. Y. Wei, J. M. Hou, L. X. Ding and H. H. Wang, *Chem. Mater.*, 2017, **29**, 7103.
30 V. M. A. Melgar, H. T. Kwon and J. Kim, *J. Membr. Sci.*, 2014, **459**, 190.
31 Y. S. Li, H. L. Chen, J. Liu and W. S. Yang, *J. Membr. Sci.*, 2006, **277**, 230.
32 Q. Wang and D. O'Hare, *Chem. Rev.*, 2012, **112**, 4124.
33 Y. Liu, N. Y. Wang, L. Diestel, F. Steinbach and J. Caro, *Chem. Commun.*, 2014, **50**, 4225.
34 Y. Liu, N. Y. Wang, J. H. Pan, F. Steinbach and J. Caro, *J. Am. Chem. Soc.*, 2014, **136**, 14353.
35 Y. Liu, J. H. Pan, N. Y. Wang, F. Steinbach, X. L. Liu and J. Caro, *Angew. Chem., Int. Ed.*, 2015, **54**, 3028.
36 Z. P. Liu, R. Z. Ma, M. Osada, N. Iyi, Y. Ebina, K. Takada and T. Sasaki, *J. Am. Chem. Soc.*, 2006, **128**, 4872.
37 Z. M. Bai, Z. Y. Wang, T. G. Zhang, F. Fu and N. Yang, *Appl. Clay Sci.*, 2012, **59–60**, 36.
38 R. Mathur and H. Lal, *J. Phys. Chem.*, 1959, **63**, 439.
39 S. S. Chen, M. Chen, S. Takamizawa, P. Wang, G. C. Lv and W. Y. Sun, *Chem. Commun.*, 2011, **47**, 4902.
40 Y. S. Li, H. Bux, A. Feldhoff, G. L. Li, W. S. Yang and J. Caro, *Adv. Mater.*, 2010, **22**, 3322.
41 A. van der Drift, *Philps Res. Rep.*, 1967, **22**, 267.
42 A. Schejn, L. Balan, V. Falk, L. Aranda, G. Medjahdi and R. Schneider, *CrystEngComm*, 2014, **16**, 4493.
43 Y. Y. Mao, W. Cao, J. W. Li, L. W. Sun and X. S. Peng, *Chem. – Eur. J.*, 2013, **19**, 11883.

